The reactivity of peroxymonosulfate towards sulfamethoxazole

Ilaria Berruti [a], Maria Inmaculada Polo López [a,b,*], Isabel Oller [a,b], Enzo Laurenti [c], Marco Minella [c,**], Paola Calza [c]

[a] CIEMAT-PSA, Carretera de Senés Km 4, 04200 Tabernas, Almería, Spain
[b] CIESOL, Joint Centre of the University of Almería-CIEMAT, 04120 Almería, Spain
[c] Department of Chemistry and NIS Inter-departmental Research Centre, Università di Torino, Via Pietro Giuria 5, 10125 Turin, Italy

ABSTRACT

In this study, an in-depth assessment of the peroxymonosulfate (PMS) reactivity towards sulfamethoxazole (SMX) is reported for the first time based on (*i*) a comparative kinetics of SMX recorded under different sources of light (simulated solar irradiation and UV-C) and in the dark, all under different operational conditions (PMS and SMX dosages, pHs, temperatures, presence of chloride and hydrogen carbonate ions) and (*ii*) monitoring the role of Reactive Oxygen Species (ROS) involved in each investigated case with the use of proper scavengers together with the recording of Electron Paramagnetic Resonance spectra. SMX degradation rates obtained in dark, at acid/neutral pH and in presence of selective ROS scavengers demonstrated that $SO_4^{\bullet-}$, $^1O_2$ and $HO^\bullet$ played a minor role; while the degradation at different pHs suggested the presence of two operational mechanisms: direct oxidation of the substrate by direct electron transfer between PMS and SMX and indirect oxidation through $HO^\bullet$ and $^1O_2$ at basic pH. Moreover, thermal assessment in dark showed that the process followed the Arrhenius equation with an activation energy 36.0 ± 1.6 kJ/mol. Under artificial solar irradiation, the kinetics constant of SMX increased due to the reached temperature and similar results were obtained in the dark at the same temperature. Therefore, the solar light could be discarded as PMS photochemical activation method for ROS generation. On the contrary, SMX degradation activated by the 254 nm PMS photolysis was based on the homolytic cleavage of the O-O bond with the formation of $SO_4^{\bullet-}$ and $HO^\bullet$ radicals with a ratio 1.2:1. $HO^\bullet$ radicals prevails over $SO_4^{\bullet-}$ at basic pH where the oxidation of OH^- to $HO^\bullet$ by $SO_4^{\bullet-}$ is strongly favored. The findings obtained in this research stands out the basis of PMS reaction in water and the mechanisms governing the microcontaminants degradation in function of the type of irradiation source and under the most commonly natural occurring inorganic water constituents, demonstrating also the potential application of this oxidant in combination with natural sunlight for water purification.

1. Introduction

Among Advanced Oxidation Processes (AOPs), the exploitation of persulfate (PS, $S_2O_8^{2-}$) or peroxymonosulfate (PMS, HSO_5^-) has been recently reconsidered as a promising technology for water purification. Typically, the activation of PS and PMS requires ultrasounds, transition metals, heat, change of pH, presence of carbon-based material or UV-C irradiation; it leads to the formation of sulfate radicals ($SO_4^{\bullet-}$), hydroxyl radicals ($HO^\bullet$) and/or other reactive oxygen species (ROS) (e.g., $^1O_2$), capable of efficiently removing organic contaminants and inactivating waterborne pathogens [1,2].

The possibility to produce active species via non-activated PMS-based processes is a particularly newsworthy alternative recently explored for water treatment, showing promising results against contaminants of emerging concern (CECs) [3] and pathogens [4]. Despite the increasing interest toward PMS applications, literature provides investigation on some of the parameters affecting the process, but the whole picture is still ambiguous and not well investigated. Yang et al. studied the degradation of different organic contaminants by PMS at pH 9 and in phosphate buffer [3]. Nihemaiti et al. investigated Ciprofloxacin and Enrofloxacin degradation in the presence of PMS at different pHs and noticed an enhanced efficiency by increasing pH, the highest performance was obtained at pH 9. The lower rates observed at pH > 9 were attributed to the formation of SO_5^{2-} as the main oxidant species in

solution, with a lower oxidant capacity compared to HSO_5^- [5]. Qi et al. demonstrated that singlet oxygen ($^1O_2$) and superoxide radical anion ($O_2^{\bullet-}$) are the predominant ROS using PMS alkaline activation; specifically, $HO^\bullet$ could be generated via the homolytic cleavage of the O-O bond of HSO_5^- [6]. Ao and co-workers investigated the sulfamethoxazole removal under medium pressure UV irradiation in the presence of PMS concluding that $SO_4^{\bullet-}$ was the major reactive species at acidic and neutral pH, while $HO^\bullet$ was the predominant reactive species in alkaline conditions. [7,8] Besides, the role played by inorganic ions commonly present in natural water, namely chloride and carbonates/bicarbonates ions, in PMS process is crucial [4,8,9] and deserves an in-depth study.

Moreover, focused on the photo-activation of PMS or PS, sulfate radicals based AOPs has been traditionally associated to the use of UV-C lamp, due to its high capability to promote the generation of ROS, while the potential application of natural sunlight has not been widely investigated and commonly it has been relegated to the use of persulfate (PS) [10]. Nevertheless, and recently, the capability of PMS (a powerful oxidative agent with $E° = 1.8$ V vs NHE) has been demonstrated in different types of water matrices and for both decontamination and disinfection. Recently, a very good and efficient degradation of organic pollutants (> 80% removal of sulfamethoxazole, diclofenac and trimethoprim in 45 min) and inactivation of several waterborne pathogens (> 5 Log reduction values of *Escherichia coli*, *Enterococcus faecalis* and *Pseudomonas aeruginosa* in 30 min) have been reported in isotonic water (demineralized water containing NaCl at 0.9% (w/v)) and under natural sunlight. However, the mechanisms governing the reactivity of PMS alone and specifically in combination with natural sunlight, is still not well understood [4].

Therefore, in the present work, a comprehensive study has been undertaken with the aim to give insights into the mechanism of PMS reactivity. For this purpose, sulfamethoxazole (SMX) has been used as model substrate and its transformation promoted by PMS in the dark, under simulated solar irradiation and under UV-C at different conditions, including diverse dosages of PMS and SMX, pHs, temperatures, presence of chloride and hydrogen carbonate ions, has been investigated. The use of tailored scavengers and the employment of Electron Paramagnetic Resonance (EPR) were applied with the goal to unravel the nature of the reactive species, with particular attention to the radical species involved in the process as a function of the different parameters. The results derived from this comparative study, which under the authoŕs knowledge has not been reported in an in-depth analysis, clearly stated the potential capability of PMS alone, both in the presence and absence of an irradiation source of light (with particular emphasis to the solar irradiation), to effectively degrade organic compounds and particularly SMX, giving clear findings on the reactive species involved and the reaction mechanism occurring in water.

2. Materials and methods

2.1. Chemicals

The commercial triple potassium salt $KHSO_5 \cdot 0.5KHSO_4 \cdot 0.5K_2SO_4$ (Oxone®, from Sigma-Aldrich) was used as source of PMS. Acetonitrile (ACN, gradient grade), H_3PO_4 (85%), sulfamethoxazole (> 99%), methanol (MeOH), tert-butanol (TBA), NaN_3, furfuryl alcol (FFA), NaCl, $NaHCO_3$, trimethoprim (TMP), phenol, 3-chloroaniline and 2,2,6,6-tetramethyl-4-piperidinol (TEMP, 99%) were purchased from Sigma-Aldrich. 5,5-dimethyl-1-pyrroline (DMPO) was obtained from Enzo Life Sciences, Inc. All the compounds were used as received. The water solutions were prepared with water of MilliQ grade (Total Organic Carbon = 2 µg/L, conductivity = 18.2 MΩ cm).

2.2. Analytical determinations

The concentrations of SMX and TMP were measured through a YL HPLC system 9300. The following conditions were used: C-18 analytical column (RP C18 LiChroCART®-LiChrosphere® with 5 µm particles), 50 µL of injection volume and flow rate at 1 mL/min with H_3PO_4 4.4 mM/ MeOH 75/25 and H_3PO_4 4.4 mM/ACN 40/60 for SMX and TMP, respectively. SMX was detected at 267 nm (retention time 7.3 min), while TMP at 273 nm (retention time 6.2 min).

The degradations obeyed first order kinetics. The concentration profiles were easily linearized ($\ln\left(\frac{C_t}{C_0}\right) = -kt$, where C_0 and C_t are the concentrations of the substrate at the time zero (i.e., the nominal concentration) and after the time t, respectively), to obtain the k values (first order degradation constants) and the related initial degradation rates ($Rate = k \times C_0$).

PMS concentration was monitored using a spectrophotometric method, based on the oxidation of the N,N′-diethyl-p-phenylenediamine (DPD). The absorbance of the sample was measured at 530 nm with a UV-Vis spectrophotometer Evolution 220 (Thermo scientific, Massachusetts, USA), after mixing 5 mL of the sample with the contents of one DPD Total Chlorine Powder Pillow, and waiting for 3 min.

2.3. Experimental procedure

All experiments were conducted in MilliQ water with an initial concentration of SMX or TMP of 1×10^{-5} M. After addition of required reagents (phosphate buffer, NaCl, $NaHCO_3$ or radical scavengers required for each operational condition) and proper homogenization in the dark, a sample was taken as control (to probe the right initial concentration of SMX), then the desired concentration of PMS was spiked, Time 0 min sample was collected and reactor was kept under (*i*) darkness at room temperature (≈25 °C), (*ii*) UV-C radiation using a Philips TUV PL-S 9 Watt Hg-lamp (254 nm of peak wavelength) placed over a 200 mL-magnetically stirred beaker or (*iii*) simulated sunlight using a CO.FO.ME.GRA Solarbox system (Italy) equipped with a Xenon arc lamp (1500 W) and a cut-off at 280 nm in a 5 mL-Pyrex glass cells (dimensions: 4.0 cm diameter and 2.5 cm height; cut-off at 295 nm).

The irradiance (39.3 ± 0.8 W/m^2) was measured with a radiometer (CO.FO.ME.GRA, Italy) from 295 to 400 nm. Water samples were frequently collected for SMX or TMP quantification, and they were supplemented with 60 µL of NaN_3 0.25 M to quench the remaining PMS. All the results showed high replicability, with relative standards deviation (RSD %) below 5%. Water temperature reached 52 ± 1 °C after few minutes of operation and the pH dropped to a value of 3, which is attributed to the OXONE® composition (HSO_5^-: HSO_4^-: SO_4^{2-} = 2:1:1) and the release of the weak acid HSO_4^- (pK$_a$ = 2) [11]. In any case, after the initial quick change both parameters (temperature and pH) remained constant during all the experimental time.

On the other hand, when pH and temperature required adjustment, phosphate buffer (4.4×10^{-3} M) and a thermostatic bath were employed, respectively.

2.4. Radical scavengers

To investigate the contribution of each active specie in the different processes involving PMS, scavenger experiments were performed with different quenching agents. TBA and MeOH were performed to highlight the specific contributions of $HO^\bullet$ and $SO_4^{\bullet-}$ radicals. TBA reacts mainly with $HO^\bullet$ ($k_{HO\bullet,TBA} = 6 \times 10^8$ M^{-1} s^{-1} [12], ≈700 times higher than that with $SO_4^{\bullet-}$, $k_{SO4-\bullet,TBA} = 8.4 \times 10^5$ M^{-1} s^{-1} [13,14]), while MeOH is an effective scavenger toward both $HO^\bullet$ and $SO_4^{\bullet-}$ ($k_{HO\bullet,MeOH} = 9.7 \times 10^8$ M^{-1} s^{-1} and $k_{SO4-\bullet,MeOH} = 1 \times 10^7$ M^{-1} s^{-1}) [13–15]. FFA and N_3^- are usually applied as scavengers for $^1O_2$ in photo-assisted processes [16]. Furthermore, N_3^- could also directly react with PMS by donating an electron. Finally, phenol and 3-chloroaniline were employed as scavengers for $Cl^\bullet$/ $Cl_2^{\bullet-}$ and $CO_3^{\bullet-}$, respectively.

2.5. Electron Paramagnetic Resonance (EPR)

EPR spectra were recorded at room temperature with a X-band Bruker EMX spectrometer equipped with a cylindrical cavity. Two spin-trapping agents were added to the cell before irradiating: DMPO (1.7×10^{-2} M) to detect $HO^{\bullet}$, $SO_4^{\bullet-}$ or $O_2^{\bullet-}$, and TEMP (1.7×10^{-2} M) for $^1O_2$ [17]. Measurements were carried out in quartz capillary tubes and the following parameters were set: microwave frequency, 9.86 GHz; microwave power, 2.7 mW; modulation frequency, 100 kHz; modulation amplitude, 2 Gauss; time constant, 0.01 ms.

When necessary, EPR spectra were simulated by the Spinfit module (included in the Bruker's Xenon software package) to identify the radical adducts.

3. Results and discussion

3.1. PMS reactivity under dark conditions

3.1.1. PMS dosage

Fig. 1a shows the SMX degradation profiles in the dark at room temperature and with different initial PMS concentrations (from 2.5×10^{-4} M to 2.0×10^{-3} M), chosen based on previous works [3,18]. All the degradation profiles followed an exponential decay and the linear trend for the degradation constant of SMX vs $[PMS]_0$ (Fig. S1a in supplementary material SM) shows a second order kinetic constant value of 0.096 ± 0.005 $M^{-1}s^{-1}$. From these results, the initial PMS concentration of 1.0×10^{-3} M was selected as the best concentration to analyze the influence of other parameters, including the scavenger tests and the oxidant reactivity. Under this condition, PMS concentration was always in excess with respect to the substrate concentration and consequently PMS was never a limiting factor for the observed processes. This is shown in Fig. S2 where the PMS concentration was monitored in the different conditions investigated in this study with an initial concentration of SMX at 1×10^{-5} M and in the same explored time interval. In all the cases the PMS concentration did not reach the zero, proof that there was always a large excess of PMS during the entire experiments here reported.

Fig. 1b shows SMX degradation profiles in the dark by PMS in the presence of MeOH, TBA, FFA and NaN_3 as scavengers, while corresponding constants rates are reported in Table S1. The addition of NaN_3 completely quenched SMX degradation in agreement with Yang et al., that reported PMS consumption in the presence of NaN_3. NaN_3 could directly react with PMS by donating an electron or with $^1O_2$ [3]. Non-radical pathway, involving PMS direct oxidation occurred and degradation inhibition in the presence of NaN_3 confirms this statement. A direct electron transfer reaction is thermodynamically permitted and

occurred according to the reaction R1 (SM). The inhibition of the transformation of SMX with PMS in the presence of NaN_3 was the result of the competition between the reaction of SMX and PMS and that of PMS and NaN_3 (that is 15 and 1500 times the initial concentration of PMS and SMX, respectively).

Furthermore, results showed that the addition of MeOH, TBA and FFA scarcely affected SMX degradation, suggesting that neither $HO^{\bullet}$, $^1O_2$ or $SO_4^{\bullet-}$, if largely formed, were the key responsible for SMX oxidation under dark conditions, as it has been also reported elsewhere [3].

3.1.2. Water temperature

Fig. 2a shows the degradation profiles of SMX with PMS (1×10^{-3} M) in the water temperature range from 20° to 70°C, to investigate the role of the temperature on the oxidant reactivity. In addition, the SMX degradation alone at 70 ºC was conducted, and results show that SMX in the absence of the oxidant is stable. Nevertheless, a significant increase of the reaction rate was observed from the lowest (20 °C, initial reaction rate = $(6.0 \pm 0.3) \times 10^{-8}$ M min^{-1}) to the highest (70 °C, initial reaction rate = $(5.0 \pm 0.2) \times 10^{-7}$ M min^{-1}) temperature. To evaluate the activation energy of the process the data were fitted through the Arrhenius equation and an activation energy equal to 36.0 ± 1.6 kJ mol^{-1} was obtained from the linear fitting of the Arrhenius plot (Fig. S1b). This value is quite similar to that reported by Qi et al. for the alkaline activated PMS degradation of acid orange 7 (AO7) [6], while it is significantly lower than the activation energy reported for the same reaction, but without the alkaline activation. The initial pH of the solution of PMS 1×10^{-3} M and SMX 1×10^{-5} M was 3. Being the activation energy of the reaction between SMX and PMS similar to that observed for the reaction of PMS and AO7, but in basic media where the quite efficient alkaline activation mechanism for PMS is operational, it can be concluded that PMS - also in dark condition - is an efficient oxidant for the removal of SMX (and presumably for similar molecules).

3.1.3. Water pH

Both PMS and SMX have acid-basic properties and pH strongly affects their speciation. The pK_a of these compounds together with the graphical representation of their acid-basic speciation are reported in Fig. S3. PMS at the pH of the common urban wastewater effluents ($\approx$ 7–8) is in its mono-anion form (HSO_5^-), at pH > 9.4 its fully deprotonated form (SO_5^{2-}) is the prevailing one and the first acid dissociation of peroxymonosulfuric acid (Caro's acid, H_2SO_5) is $pK_{a1} = 0.4$ [19]. For SMX, the mono-cationic form prevails at pH < 1.6, while the mono-anionic form at pH > 5.7. Furthermore, the redox potential of the oxidant and/or of the reactive species generated can change as a function of the pH.

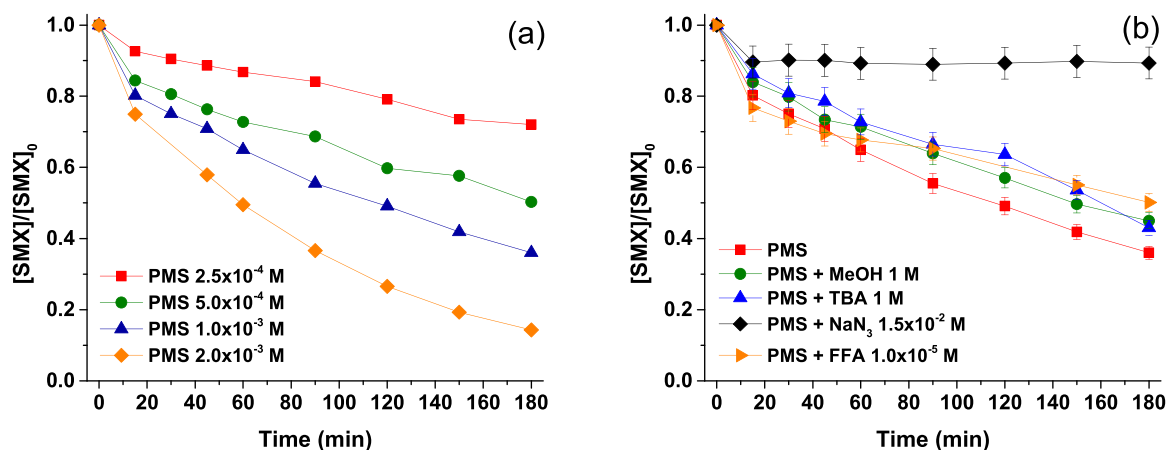Fig. 2b shows SMX degradation profiles by PMS in the pH interval

Fig. 1. SMX degradation profiles under dark conditions at r.t. and pH 3, by: (a) different concentrations of PMS (2.5×10^{-4}, 5.0×10^{-4}, 1.0×10^{-3} and 2.0×10^{-3} M) and b) PMS (1.0×10^{-3} M) in the presence of radical scavengers.
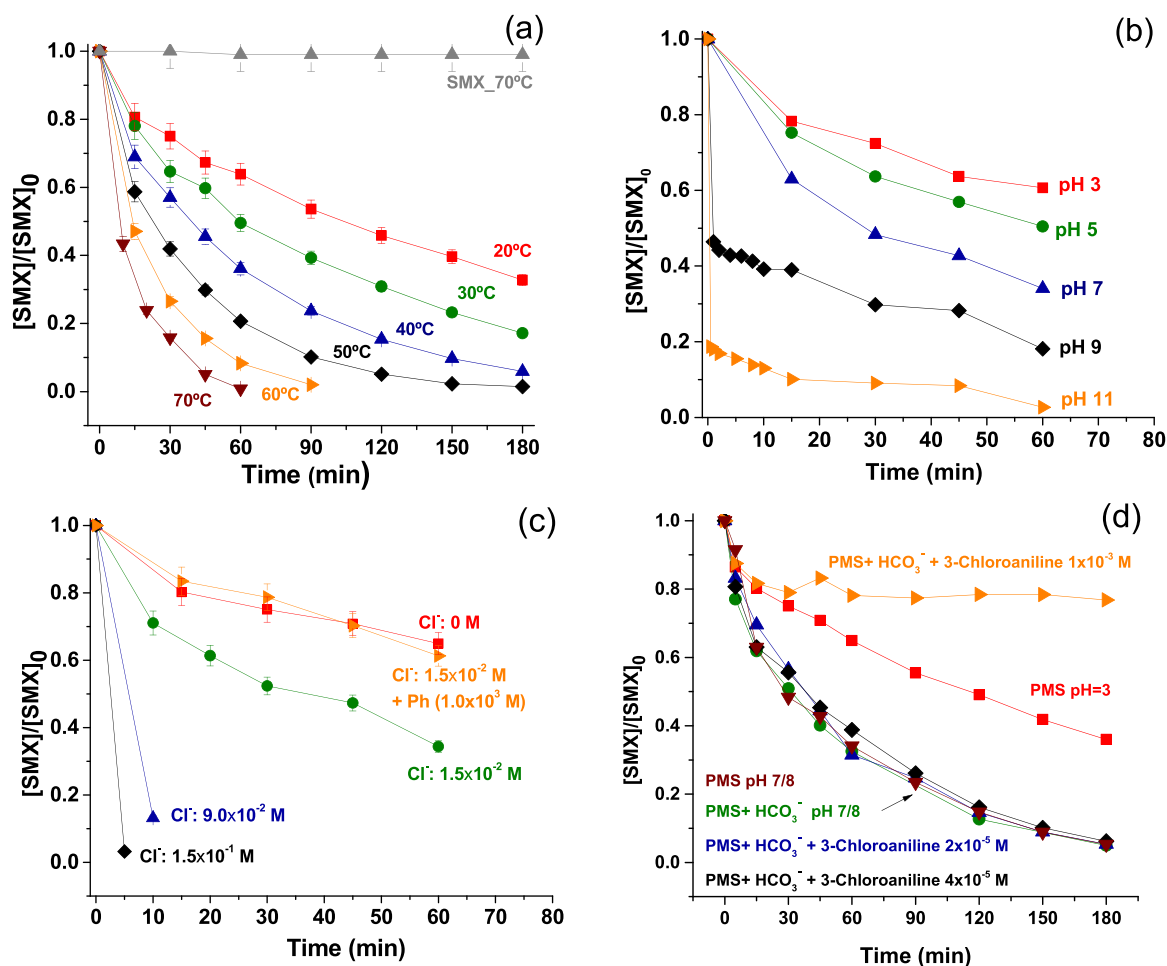
Fig. 2. SMX degradation by PMS 1.0×10^{-3} M in the dark: (a) at different temperatures (from $20°$ to $70°$C) at pH 3, (b) at different pHs (from 3 to 11) at r.t, (c) different Cl^- concentrations (0, 1.5×10^{-2}, 9.0×10^{-2} and 1.5×10^{-1} M) and with phenol 1.0×10^{-3} M, and (d) with HCO_3^- (4.0×10^{-3} M) and in the presence of different concentrations of 3-Chloroaniline (2.0×10^{-5}, 4.0×10^{-5} and 1.0×10^{-3} M), and alone at pH 7 for phosphate buffer.

3–11. The mere effect of pH was also investigated, and no significant removal was observed in any case (data not shown), in good agreement with literature [3]. Nevertheless, the increase of the pH changed the kinetics of SMX degradation in the presence of the oxidant. At acidic pH (3 and 5) a single exponential decay was observed, while from pH 7 and especially at pH 9 and 11, a double kinetics was manifest, with a sharp decrease of the SMX concentration immediately after the oxidant addition, accordingly with the production of ROS, followed by a progressive exponential decay up to the complete degradation.

The mono-anionic SMX specie is the mainly involved specie in the reaction at pH 7–11 and it reacts faster than the neutral and cationic ones with both $HO^\bullet$ and $^1O_2$ (see Table S2 [20]). Nihemaiti et al., investigated the degradation of ciprofloxacin and enrofloxacin with PMS alone and observed the maximum degradation rate of these two fluoroquinolones at pH around 9, as a balance between the formation of the most reactive species (the deprotonated forms) and the presence of HSO_5^- with a higher oxidant capacity with respect to SO_5^{2-}, that prevails at pH > 9.4 [5]. Note that, in agreement with the Nernst equation, the formal redox potential for the couple HSO_5^-/SO_4^{2-} decreases ≈ 30 mV per pH unit up to pH = 9.4 and 59 mV per pH unit at higher pH (considering the semireactions R2 and R3 in SM).

Furthermore, $^1O_2$ and $O_2^{\bullet-}$ have been proposed as the predominant ROS during the alkaline activation of PMS [6].

The data reported in Fig. 2b suggest a possible overlapping of two mechanisms for the dark degradation of SMX by PMS: from one hand, the direct oxidation of the substrate promoted by the direct electron transfer between PMS and the SMX, and on the other hand its indirect

oxidation (e.g., reaction mediated by $HO^\bullet$ and $^1O_2$, vide infra) that prevails at basic pH. Further and more specific analysis in this experimental conditions are needed to confirm which is the relative weight of the two mechanisms.

3.1.4. Role of inorganic ions

The degradation of SMX was investigated at different concentrations of both Cl^- and HCO_3^- (Fig. 2c-d), not only to highlight possible interferences of these inorganic species in a real treatment scenario, but also to give insights into the operative transformation mechanism activated in the dark by PMS.

The data obtained with Cl^- (Fig. 2c) suggested that the main mechanism of transformation of organic compounds by PMS (at acid pH) was the direct oxidation of the substrate by $Cl_2/HClO$ formed by the PMS bielectronic oxidation of the Cl^- (vide infra). Note that the same mechanism could be silent at basic pH. At the maximum investigated Cl^- concentration, SMX immediately dropped down to zero in the first minutes after the oxidant addition. An operative role of active (oxidative) chlorine species can be easily hypothesized. At pH 3 (the natural pH of the SMX, PMS and NaCl solutions here tested) the formal standard potential for the couple HSO_5^-/SO_4^{2-} (R2) is roughly 1.7 V vs NHE, sufficiently high to promote the production of active chlorine and in particular $Cl_2/HClO$ (R4, R5, R6 in SM) [21], while it is not able to promote the formation of the radical $Cl_2^{\bullet-}$ (R7 in SM) [22]. Zhou et al. also observed an accelerated degradation of steroid estrogens in the presence of both Br^- and Cl^- (at environmentally relevant concentrations) with the formation of halogenated aromatic products [23]. Berruti

et al. compared the rate of transformation of a CECs mixture in ultrapure and isotonic water observing a significant increment of the removal rate in the latter matrix [4]. On the contrary, Nihemaiti et al. did not observe any effect on the transformation rate of ciprofloxacin in the presence of Cl^- 5.0×10^{-3} M, but at pH 8.2 for borate buffer [5]. This is in agreement with the lower oxidative properties of the ClO^- (R5 in SM) with respect to the HClO ($pK_a = 7.52$) [21]. In addition, the presence of phenol decreased more than 3 times SMX degradation (the transformation rates were $(7.0 \pm 0.2) \times 10^{-8}$ M min^{-1} and $(2.2 \pm 0.2) \times 10^{-7}$ M min^{-1} in the presence and absence of phenol, respectively). Phenol and phenolic compounds are effective scavengers of the active chlorine, being easily monoelectronically oxidized by HClO (especially at acidic pH) [24]. The E° for the couple phenoxyl radical/ phenol is 1.28 V vs NHE at pH 3 [25]. Furthermore, the addition of HCO_3^- (4.0×10^{-3} M) increased the reaction rate 3-times with respect to the experiment with PMS alone (Fig. 2d), suggesting that the role of HCO_3^- could be either as pH modifier (by adding HCO_3^- water pH increased to pH 7) or as source of $CO_3^{\bullet-}$. Chloroanilines were used as substrates easily to be oxidized and high reaction rate constants with carbonate radical are reported [22]. Similar SMX degradation profiles were obtained, comparing the experiments with 4.0×10^{-3} M of HCO_3^- in MilliQ water alone, with 3-chloroaniline (at 2.0×10^{-5} or 4.0×10^{-5} M) and in phosphate buffer at pH 7 (in the absence of HCO_3^-), highlighting an important effect of pH on the reaction rate increase. On the other hand, the significant decrease in SMX degradation rate in the presence of 3-chloroaniline 1.0×10^{-3} M could be related not to a scavenger effect towards $CO_3^{\bullet-}$, but toward PMS, that at this concentration reacted mainly with 3-chloroaniline than with SMX. Therefore, from the data emerged that in the explored experimental conditions an active role of the $CO_3^\bullet$ for SMX degradation could be excluded. Similarly, Nihemaiti et al. observed that the degradation of ciprofloxacin with PMS (5.0×10^{-6} M) was not affected by HCO_3^- (5.0×10^{-3} M) (experiments were carried out at the same pH) [5].

3.2. PMS reactivity under solar irradiation

Fig. 3a collects SMX degradation profiles under simulated solar light, showing that only 25% was degraded after 90 min with direct photolysis, while the addition of PMS (1.0×10^{-3} M) leads to the abatement of 90% of SMX in the same treatment time. Results obtained following the addition of MeOH and TBA as scavengers showed only a very slight inhibition, suggesting that also under simulated solar radiation neither $HO^\bullet$ nor $SO_4^{\bullet-}$ radicals were the main responsible of SMX oxidation. Temperature reached inside the sun simulator was around 50 °C and, interestingly, the enhancement in the degradation efficiency under simulated solar light closely resemble the one obtained in the dark at the same temperature; the degradation rates remained the same also after the addition of scavenger in the dark (Fig. S4 and Table S2). These data prompted to conclude that PMS direct oxidation of SMX under sunlight can be merely attributed to a thermal effect (i.e., an increase of T in the reactor), in agreement with the absence of overlap between the emission spectrum of the lamp employed and the absorption spectra of PMS, directly discarding the activation of PMS for radicals generation [26].

3.3. PMS reactivity under UV-C light

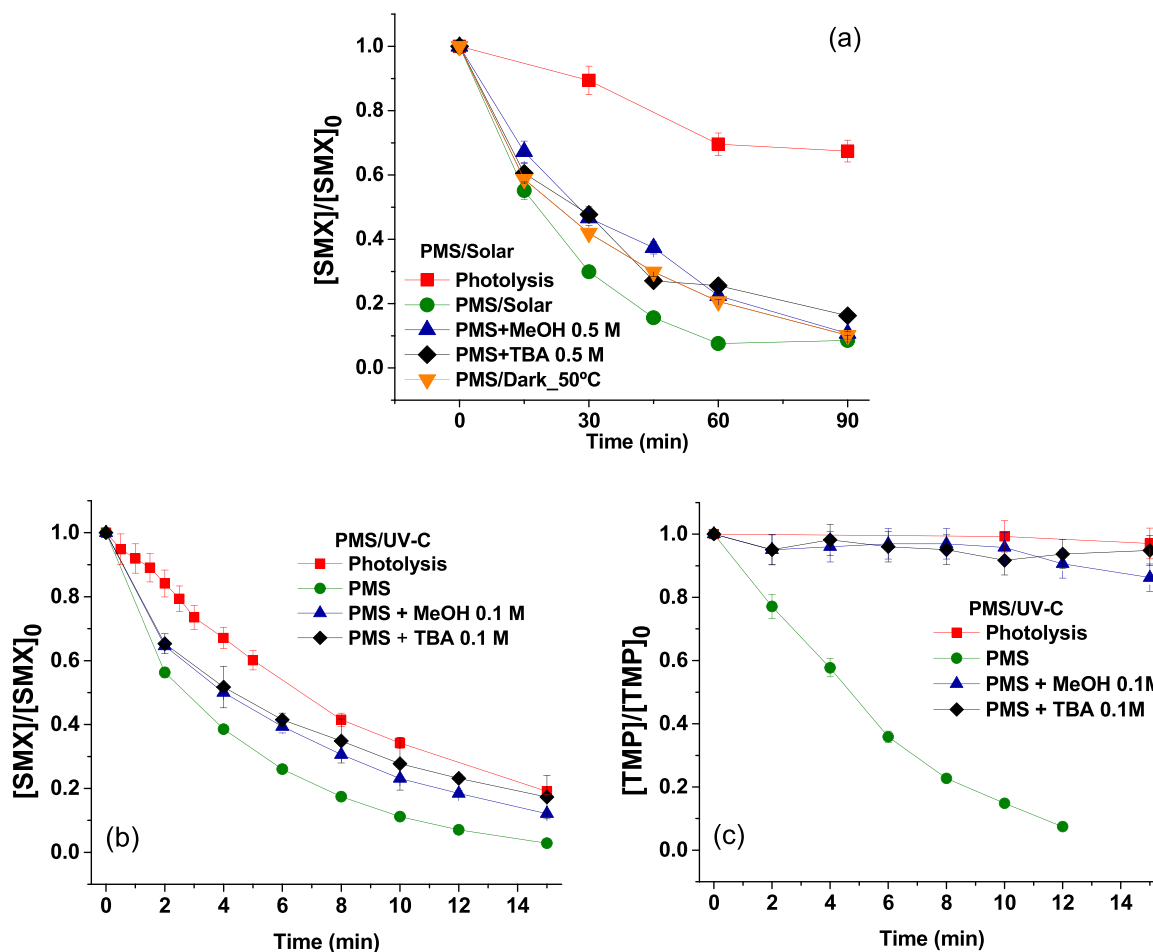Under UV-C irradiation, SMX underwent direct photolysis, leading to

Fig. 3. (a) SMX degradation by PMS (1×10^{-3} M) with and without ROS under simulated solar radiation, and under dark conditions at 50 °C for comparison and (b) and (c) SMX and TMP degradation profiles under UV-C light in the presence of PMS (3×10^{-3} M) and MeOH 0.1 M or TBA 0.1 M, respectively.

80% of removal after 15 min, while almost complete disappearance of SMX was observed after the addition of PMS 3.0×10^{-3} M (concentration chosen in an attempt to strengthen the role of PMS) (Fig. 3b). To avoid the effect of photolysis on the reactivity analysis of PMS, a substrate less prone to be direct photolysed by UV-C, as TMP, was investigated (Fig. 3c). The photolysis of TMP was negligible, while the addition of PMS lead to its degradation in a few minutes. The introduction of scavengers largely quenched the degradation of TMP, so highlighting that UV-C irradiation was capable to activate the homolytic cleavage of the peroxide bond in PMS generating $SO_4^{\bullet-}$ and $HO^{\bullet}$ radicals in solution, playing a strong role during TMP degradation by the 254-nm photolysis of PMS.

3.4. EPR detection

The intensity of the EPR signals with DMPO increased in the order dark < solar light < < UV-C irradiation. Fig. S5 shows EPR spectra obtained after 10 min irradiation of PMS under UV-C light together with the correspondent simulation, highlighting the presence of two radical species that can be assigned to DMPO-HO$^{\bullet}$ (a_N = 15.0 Gs; a_H = 14.7 Gs) and DMPO-SO$_4^{\bullet-}$ (a_N = 13.9 Gs; a_H = 9.7 Gs) adducts [27,28]. Both the patterns attributable to the presence of $SO_4^{\bullet-}$ and $HO^{\bullet}$ were observed in all solutions containing PMS even if, in the dark, the signals were very low (compare the spectra reported in Fig. S5, S6a and Fig. 4a). Moreover, the simulation of EPR spectra permitted to observe that, in our experimental conditions, the ratio DMPO-SO$_4^{\bullet-}$/DMPO-HO$^{\bullet}$ was quite independent from the type and intensity of irradiation and it was estimated in 1.2:1 (standard deviation 3%). On the other hand, experiments at pH 11 revealed an enhancement of the production of HO$^{\bullet}$ imputable to the higher ability of $SO_4^{\bullet-}$ to oxidize water/hydroxyl anion in more basic conditions than at circumneutral/acid pH (Fig. S6b), whereas EPR patterns due to DMPO-HO$^{\bullet}$ and DMPO-SO$_4^{\bullet-}$ adducts almost disappeared in experiments where NaN$_3$ was added to the reaction mixture. In this case an intense signal of the DMPO-N$_3^{\bullet}$ adduct ($a_{N(NO)}$ = 14.7 Gs; a_H = 14.2 Gs; $a_{N(N3)}$ = 3.1 Gs [29] was recorded (Fig. S6c) and only the

simulation of the experimental spectra revealed the presence of a weak signal of the DMPO-HO$^{\bullet}$ adduct (Fig. S6d). From the simulation, a ratio DMPO-N$_3^{\bullet}$/DMPO-HO$^{\bullet}$ around to 10:1 was calculated, confirming the quenching effect of N$_3^-$ previously observed. In the absence of PMS, no EPR signal was recorded in the presence of DMPO and NaN$_3$ alone.

In the presence of Cl$^-$, EPR analysis revealed the presence of intense spectra attributable to 5,5-dimethyl-2-pyrrolidone-N-oxyl (DMPOX, a_N = 7.2 Gs; $2a_H$ = 4.1 Gs) (Fig. 4b) [30]. This is consistent with the presence of a high concentration of active chlorine, which was probably responsible for the dependence from Cl$^-$ concentration of SMX oxidation showed in Fig. 2c.

DMPOX formation was also observed when a PMS solution was irradiated under simulated solar light in the presence of DMPO (Fig. 4a). In this case, the EPR patterns of DMPO-HO$^{\bullet}$ and DMPO-SO$_4^{\bullet-}$ adducts, observed by irradiating for a few minutes, were progressively substituted by DMPOX spectrum, this is coherent with a progressive enhancement of the oxidation induced by long-time irradiation (more than 15 min) [31]. As reported above, the main transformation mechanism under simulated solar irradiation was not the homolytic cleavage of the peroxide bond of PMS and consequently, an indirect oxidation mediated by radical species, but the direct electron transfer promoted by the interaction of PMS with the substrate, in this case the spin trap.

Addition of TEMP to PMS solutions permitted to reveal the formation of the typical three-lines EPR spectrum, characteristic of 4-oxo-2,2,6,6-tetramethyl-1-piperidinyloxy radical, resulting from the addition of singlet oxygen to the nitrogen atom in TEMP (Fig. 4c). The presence of this specie was recorded in all the experiments, indicating the formation of $^1O_2$ in all the tested conditions. At pH 11 the concentration of $^1O_2$ was particularly high (Fig. 4d), in agreement with the noteworthy production of $^1O_2$ during the alkaline activation of PMS [6]. Furthermore, identical spectra in the dark and at pH 3 were obtained in the presence of dissolved oxygen and under anoxic conditions (compare Fig. 4c and Fig. S7a), this proved that $^1O_2$ was formed by the decomposition of PMS and not from the reaction of PMS with the dissolved oxygen. In the presence of increasing concentrations of NaN$_3$, the EPR TEMPO signal
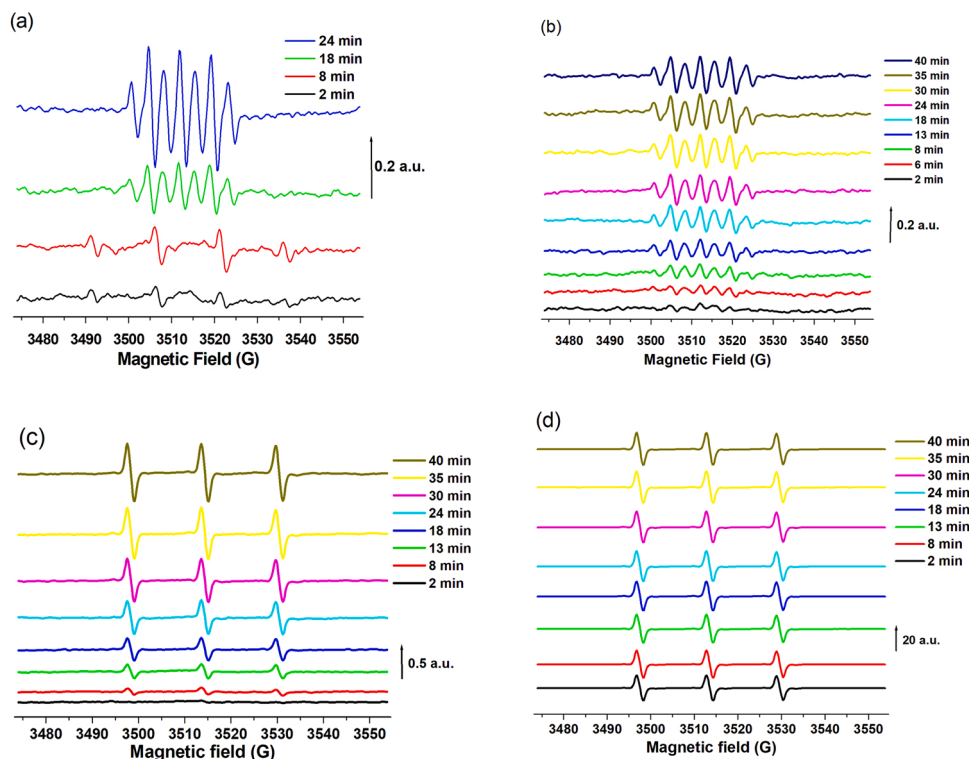

Fig. 4. EPR spectra of DMPOX (a) under simulated sunlight and (b) in the dark with Cl$^-$ 1.5×10^{-1} M, and of TEMP adducts formed by PMS in the dark (c) at pH = 3 and (d) at pH = 11 formed at different times by PMS (3×10^{-3} M).

decreased in agreement with the quenching ability of the N_3^- toward $^1O_2$ (Fig. S7b-c). No signal was recorded during the control experiment with NaN_3 and TEMP alone.

4. Conclusions

The reactivity of PMS toward SMX has been in-depth investigated to highlight the main mechanisms occurring during the degradation of this contaminant under different conditions.

It has been concluded that PMS alone in dark conditions is an efficient oxidant for the removal of SMX and in the absence of both catalytic and/or photochemical activation the process followed the Arrhenius equation with an activation energy equal to 36.0 ± 1.6 kJ/mol. The degradation profiles at different pH suggested that two transformation mechanisms were operative in dark: the direct oxidation of the substrate promoted by direct electron transfer between PMS and the SMX and the indirect oxidation through $HO^\bullet$ and $^1O_2$ (especially at basic pH where the alkaline activation produced significant amount of $^1O_2$). With Cl^-, PMS promotes the oxidation of SMX through the formation of active chlorine (e.g., $Cl_2/HClO$) especially at acid pH, while the same mechanism could be silent in alkaline conditions. On the opposite, an active role of HCO_3^- as $CO_3^{\bullet-}$ source could be excluded. The experiments in the presence of active scavenger species (e.g., MeOH, TBA, FFA and NaN_3) suggested that neither $HO^\bullet$, $^1O_2$ nor $SO_4^{\bullet-}$ were the key responsible of SMX oxidation in the dark and without any external activation step.

The increase SMX transformation rate by PMS/Solar could be attributed to increment of water temperature, discarding the photochemical activation.

SMX and especially TMP (less prone to the direct UV-C photolysis than SMX) degradation by PMS/UV-C was based on the homolytic cleavage of the O-O bond with the formation of $SO_4^{\bullet-}$ and $HO^\bullet$ radicals with a ratio 1.2:1 (experimentally evaluated comparing the EPR DMPO-$SO_4^{\bullet-}$/DMPO-$HO^\bullet$ signals). A main presence of $HO^\bullet$ with respect to $SO_4^{\bullet-}$ was observed at basic pH where the oxidation of OH^- to $HO^\bullet$ by $SO_4^{\bullet-}$ is strongly favored.

The EPR signal observed with DMPO increased in the order dark < solar light < UV-C irradiation, confirming the minor role of the sulfate radical mediated transformation mechanism of SMX by PMS in dark.

CRediT authorship contribution statement

Ilaria Berruti: Investigation, Methodology, Writing – review & editing. **M. Inmaculada Polo López**: Supervision, Writing – review & editing. **Isabel Oller**: Writing – review & editing. **Enzo Laurenti**: Methodology, Writing – review & editing. **Paola Calza**: Writing – original draft, Writing – review & editing, Funding acquisition. **Marco Minella**: Conceptualization, Writing – original draft, Writing – review & editing.

Declaration of Competing Interest

The authors declare that they have no known competing financial interests or personal relationships that could have appeared to influence the work reported in this paper.

Data availability

Data will be made available on request.

Acknowledgments

Appendix A. Supporting information

Supplementary data associated with this article can be found in the online version at doi:10.1016/j.cattod.2022.12.006.

References

[1] S. Guerra-rodríguez, E. Rodríguez, D.N. Singh, Assessment of Sulfate Radical-Based Advanced Oxidation Processes for Water and Wastewater Treatment: A Review Assessment of Sulfate Radical-Based Advanced Oxidation Processes for Water and Wastewater Treatment: A Review 4 (2018), https://doi.org/10.3390/w10121828.

[2] I. Berruti, S. Nahim-Granados, M.J. Abeledo-Lameiro, I. Oller, M.I. Polo-López, UV-C peroxymonosulfate activation for wastewater regeneration: simultaneous inactivation of pathogens and degradation of contaminants of emerging concern, Molecules 26 (2021), https://doi.org/10.3390/molecules26164890.

[3] Y. Yang, G. Banerjee, G.W. Brudvig, J.H. Kim, J.J. Pignatello, Oxidation of organic compounds in water by unactivated peroxymonosulfate, Environ. Sci. Technol. 52 (2018) 5911–5919, https://doi.org/10.1021/acs.est.8b00735.

[4] I. Berruti, I. Oller, M.I. Polo-Lopez, Direct oxidation of peroxymonosulfate under natural solar radiation: accelerating the simultaneous removal of organic contaminants and pathogens from water, Chemosphere 279 (2021), https://doi.org/10.1016/j.chemosphere.2021.130555.

[5] M. Nihemaiti, R.R. Permala, J.P. Croué, Reactivity of unactivated peroxymonosulfate with nitrogenous compounds, Water Res. 169 (2020), https://doi.org/10.1016/j.watres.2019.115221.

[6] C. Qi, X. Liu, J. Ma, C. Lin, X. Li, H. Zhang, Activation of peroxymonosulfate by base: implications for the degradation of organic pollutants, Chemosphere 151 (2016) 280–288, https://doi.org/10.1016/j.chemosphere.2016.02.089.

[7] X. Ao, W. Liu, W. Sun, C. Yang, Z. Lu, C. Li, Mechanisms and toxicity evaluation of the degradation of sulfamethoxazole by MPUV/PMS process, Chemosphere 212 (2018) 365–375, https://doi.org/10.1016/j.chemosphere.2018.08.031.

[8] X. Ao, W. Liu, Degradation of sulfamethoxazole by medium pressure UV and oxidants: peroxymonosulfate, persulfate, and hydrogen peroxide, Chem. Eng. J. 313 (2017) 629–637, https://doi.org/10.1016/j.cej.2016.12.089.

[9] Y. Sun, H. Xie, C. Zhou, Y. Wu, M. Pu, J. Niu, The role of carbonate in sulfamethoxazole degradation by peroxymonosulfate without catalyst and the generation of carbonate racial, J. Hazard. Mater. 398 (2020) 122827, https://doi.org/10.1016/j.jhazmat.2020.122827.

[10] L.C. Ferreira, M. Castro-Alférez, S. Nahim-Granados, M.I. Polo-López, M.S. Lucas, G. Li Puma, P. Fernández-Ibáñez, Inactivation of water pathogens with solar photo-activated persulfate oxidation, Chem. Eng. J. 381 (2020) 122275, https://doi.org/10.1016/j.cej.2019.122275.

[11] D.R. Lide, CRC Handbook of Chemistry and Physics, 85th Edition - Google Books, 85th ed., 2004. https://books.google.es/books?hl=en&lr=&id=WDll8hA006AC&oi=fnd&pg=PA1&dq=lide+2004&ots=U0mJ_ROUNs&sig=vh8FvABCmwKMHW5Q7E9a0r-solY&redir_esc=y#v=onepage&q=lide 2004&f=false (accessed July 21, 2022).

[12] G.V. Buxton, C.L. Greenstock, W.P. Helman, A.B. Ross, Critical Review of rate constants for reactions of hydrated electrons, hydrogen atoms and hydroxyl radicals (·OH/·O− in aqueous solution, J. Phys. Chem. Ref. Data 17 (1988) 513, https://doi.org/10.1063/1.555805.

[13] C.L. Clifton, R.E. Huie, Rate constants for hydrogen abstraction reactions of the sulfate radical, SO_4^-. Alcohols, Int. J. Chem. Kinet. 21 (1989) 677–687, https://doi.org/10.1002/kin.550210807.

[14] L. Zhou, C. Ferronato, J.M. Chovelon, M. Sleiman, C. Richard, Investigations of diatrizoate degradation by photo-activated persulfate, Chem. Eng. J. 311 (2017) 28–36, https://doi.org/10.1016/j.cej.2016.11.066.

[15] Z. Wang, K. Zhu, J. Chen, G. Zhang, W. Duo Wu, S.P. Sun, Oxone activation by UVA-irradiated FeIII-NTA complex: efficacy, radicals formation and mechanism on crotamiton degradation, Chem. Eng. J. 408 (2021), 127324, https://doi.org/10.1016/j.cej.2020.127324.

[16] L. Chen, C. Zhao, D.D. Dionysiou, K.E. O'Shea, TiO2 photocatalytic degradation and detoxification of cylindrospermopsin, J. Photochem. Photobiol. A Chem. 307–308 (2015) 115–122, https://doi.org/10.1016/j.jphotochem.2015.03.013.

[17] S. García-Ballesteros, J. Grimalt, S. Berto, M. Minella, E. Laurenti, R. Vicente, M.F. López-Pérez, A.M. Amat, A. Bianco Prevot, A. Arques, New route for valorization of oil-mill wastes: isolation of humic-like substances to be employed in solar-driven processes for pollutants removal, ACS Omega 3 (2018) 13073–13080, https://doi.org/10.1021/acsomega.8b01816.

[18] X. Yang, X. Ding, L. Zhou, Q. Zhao, Y. Ji, X. Wang, J.M. Chovelon, G. Xiu, Direct oxidation of antibiotic trimethoprim by unactivated peroxymonosulfate via a nonradical transformation mechanism, Chemosphere 263 (2021), 128194, https://doi.org/10.1016/j.chemosphere.2020.128194.

[19] J. Mao, D.J. Jacob, M.J. Evans, J.R. Olson, X. Ren, W.H. Brune, J.M. Clair St., J.D. Crounse, K.M. Spencer, M.R. Beaver, P.O. Wennberg, M.J. Cubison, J.L. Jimenez, A. Fried, P. Weibring, J.G. Walega, S.R. Hall, A.J. Weinheimer, R.C. Cohen, G. Chen, J.H. Crawford, C. McNaughton, A.D. Clarke, L. Jaeglé, J.A. Fisher, R.M. Yantosca, P. Le Sager, C. Carouge, Chemistry of hydrogen oxide radicals (HOx) in the Arctic troposphere in spring, Atmos. Chem. Phys. 10 (2010) 5823–5838, https://doi.org/10.5194/acp-10-5823-2010.

[20] L. Ge, P. Zhang, C. Halsall, Y. Li, C.E. Chen, J. Li, H. Sun, Z. Yao, The importance of reactive oxygen species on the aqueous phototransformation of sulfonamide antibiotics: kinetics, pathways, and comparisons with direct photolysis, Water Res. 149 (2019) 243–250, https://doi.org/10.1016/j.watres.2018.11.009.

[21] D. Harris, Quantitative Chemical Analysis 8th ed. (n.d.). https://www.academia. edu/32454429/Harris_Quantitative_Chemical_Analysis_8th_edition (accessed October 4, 2021).

[22] R.E.H. Neta P, Rate constants for reactions of inorganic radicals in aqueous solution, National Standard Reference Data System, 1979.

[23] Y. Zhou, J. Jiang, Y. Gao, S.Y. Pang, J. Ma, J. Duan, Q. Guo, J. Li, Y. Yang, Oxidation of steroid estrogens by peroxymonosulfate (PMS) and effect of bromide and chloride ions: kinetics, products, and modeling, Water Res. 138 (2018) 56–66, https://doi.org/10.1016/j.watres.2018.03.045.

[24] D. Vione, V. Maurino, C. Minero, P. Calza, E. Pelizzetti, Phenol chlorination and photochlorination in the presence of chloride ions in homogeneous aqueous solution, Environ. Sci. Technol. 39 (2005) 5066–5075, https://doi.org/10.1021/ es0480567.

[25] C. Li, M.Z. Hoffman, One-electron redox potentials of phenols in aqueous solution, J. Phys. Chem. B 103 (1999) 6653–6656, https://doi.org/10.1021/jp983819w.

[26] I. Berruti, S. Nahim-Granados, M.J. Abeledo-Lameiro, I. Oller, M.I. Polo-López, Recent advances in solar photochemical processes for water and wastewater disinfection, Chem. Eng. J. Adv. 10 (2022), 100248, https://doi.org/10.1016/j. ceja.2022.100248.

[27] M.L. Tummino, E. Laurenti, F. Deganello, A. Bianco Prevot, G. Magnacca, Revisiting the catalytic activity of a doped $SrFeO_3$ for water pollutants removal:

[28] G. Liu, S. You, Y. Tan, N. Ren, In situ photochemical activation of sulfate for enhanced degradation of organic pollutants in water, Environ. Sci. Technol. 51 (2017) 2339–2346, https://doi.org/10.1021/acs.est.6b05090.

[29] B. Kalyanaraman, E.G. Janzen, R.P. Mason, Spin trapping of the azidyl radical in azide/catalase/H_2O_2 and various azide/peroxidase/H_2O_2 peroxidizing systems, J. Biol. Chem. 260 (1985) 4003–4006, https://doi.org/10.1016/s0021-9258(18) 89222-5.

[30] T. Ozawa, Y. Miura, J.I. Ueda, Oxidation of spin-traps by chlorine dioxide (ClO_2) radical in aqueous solutions: first ESR evidence of formation of new nitroxide radicals, Free Radic. Biol. Med. 20 (1996) 837–841, https://doi.org/10.1016/ 0891-5849(95)02092-6.

[31] C. Giorio, S.J. Campbell, M. Bruschi, F. Tampieri, A. Barbon, A. Toffoletti, A. Tapparo, C. Paijens, A.J. Wedlake, P. Grice, D.J. Howe, M. Kalberer, Online quantification of criegee intermediates of α-pinene ozonolysis by stabilization with spin traps and proton-transfer reaction mass spectrometry detection, J. Am. Chem. Soc. 139 (2017) 3999–4008, https://doi.org/10.1021/JACS.6B10981/SUPPL_ FILE/JA6B10981_SI_001.PDF.

effect of light and temperature, Appl. Catal. B Environ. 207 (2017) 174–181, https://doi.org/10.1016/j.apcatb.2017.02.007.